IEEE Access
Multidisciplinary | Rapid Review | Open Access Journal

Date of publication xxxx 00, 0000, date of current version xxxx 00, 0000.

Digital Object Identifier 10.1109/ACCESS.2024.0429000

Enhanced Coronary Artery Disease Classification through Feature Engineering and One-Dimensional Convolutional Neural Network

ATITAYA PHOEMSUK[1], (Student Member, IEEE), VAHID ABOLGHASEMI[2] (Senior Member, IEEE)
[1]School of Computer Science and Electronic Engineering, University of Essex, Colchester, United Kingdom (e-mail: ap19698@essex.ac.uk)
[2]School of Computer Science and Electronic Engineering, University of Essex, Colchester, United Kingdom (e-mail: v.abolghasemi@essex.ac.uk)

Corresponding author: Atitaya Phoemsuk (e-mail: ap19698@essex.ac.uk).

ABSTRACT Coronary artery disease (CAD) diagnosis remains a significant contributor to global mortality rates, highlighting the need for novel approaches. Existing CAD diagnostic tools rely on costly and complex biomarkers and scanners. In this paper, using only electrocardiogram (ECG) signals, we propose a novel learning-based model for CAD diagnosis. The proposed method works based on a one-dimensional convolutional neural network (1D-CNN), offering a cost-effective alternative for sophisticated cardiac health monitoring. Furthermore, we introduce the concept of feature engineering to improve the quality of the model training process and mitigate the challenge of ill-conditioned ECG data. Unlike existing approaches, which often overlook signal quality, our model applies a smart feature engineering, ensuring that only diagnostically reliable signals are used. This design improves robustness, generalisability, and suitability for real-world clinical settings. Utilising one of the most complex publicly available datasets, i.e., MIMIC III, sourced from Physionet, the performance of the proposed model, along with existing ones in classifying potential cases of CAD and non-CAD is investigated. Our findings confirm that the proposed model exhibits outstanding performance, highlighting the effectiveness of our integrated feature engineering approach with the CNN model.

INDEX TERMS Convolutional neural networks, Electrocardiogram, Coronary artery disease, Cardiovascular disease, Myocardial infarction.

I. INTRODUCTION

Coronary Artery Disease (CAD) remains the most prevalent type of Cardiovascular Disease (CVD) and is the leading cause of death worldwide, contributing to millions of deaths annually [1]. A study indicated that CVD is anticipated to maintain its position as the foremost cause of mortality worldwide by the year 2030, with notable prevalence expected across both high and low-income nations [2]. CAD develops when cholesterol progressively accumulates, narrowing the walls of the coronary arteries. This condition gives rise to two severe manifestations: myocardial infarction and angina. Studies indicate that advanced symptoms of CAD typically display during middle age, highlighting the correlation between aging and the likelihood of CAD development [3], [4]. Hence, it is imperative to implement preventive measures and establish pre-screening protocols for high-risk patients.

CAD is typically diagnosed through various diagnostic tests, including electrocardiography (ECG), treadmill ECG, echocardiography (ECHO), and angiography. ECG is most commonly used for all CVD initial screening in general practices due to being a cost-effective and widely accessible tool, capable of facilitating continuous monitoring, portability, and ability to provide real-time data. However, the current diagnosis using ECG is conducted manually, is time-consuming, and is subject to human error, posing significant challenges in clinical practices. Hence, to address this issue, we propose an intelligent learning-based approach to improve diagnostic efficiency. The proposed model serves as a cost-effective and user-friendly pre-screening tool for patients, requiring minimal specialised medical expertise.

With the development of state-of-the-art technologies, different classical machine learning architectures are used for predicting ECG-related issues, such as Support Vector Machine (SVM) [5, 6], K-nearest neighbour (kNN) [7], K-means [8]. Furthermore, numerous deep learning techniques are employed on ECG signals to classify heart diseases. Among these, Convolutional Neural Networks (CNNs) [9], Long Short-Term Memory (LSTM) networks [10], Recurrent

Neural Networks (RNNs) [11], Residual Neural Network (ResNet) [12, 13, 14], and Autoencoders [15] have been applied to ECG signals for heart disease classification. The primary advantage of deep learning techniques is the ability to eliminate the need for feature extraction processes, unlike classical machine learning techniques that often necessitate explicit feature extraction. On the contrary, deep learning models carry out feature extraction automatically and implicitly, leveraging a robust pattern learning ability and adaptable processing architectures.

Recent studies have shown that CNN architecture is effective in various medical diagnostic tasks, such as detecting COVID-19 lesions in CT scans, diagnosing Alzheimer's disease from hippocampal MRI, classifying skin lesions in dermoscopy images, and identifying breast abnormalities in mammograms [16, 17, 18, 19]. These examples demonstrate that CNN can successfully learn important medical features from complex data, supporting disease detection, localisation, and analysis across different types of medical images. CNN has also been applied to non-imaging biomedical signals, most notably the ECG, which is widely used in the diagnosis of cardiovascular diseases [20].

A hybrid CNN-LSTM architecture is introduced for the detection of CAD, utilising anomalous ECG morphology and irregular heart rate variability (HRV) to discern CAD and non-CAD cases [9]. Additionally, the CNN-LSTM architecture is applied for CAD identification [10]. However, the diagnostic accuracy of CAD is impeded by constraints in the available data, as public resources provide only limited datasets and lack certain definitive biomarkers. Several studies have implemented 1D-CNN for the automated detection of CAD, aiming to enhance diagnostic accuracy and improve patient outcomes. In [21], an automated CAD diagnosis system utilising 1D-CNN is presented, showcasing notable outcomes in accuracy and computational efficiency. The 1D-CNN approach effectively distinguished between CAD and non-CAD subjects. The integration of feature extraction techniques into their proposed model yielded promising accuracy levels. Nevertheless, the training process of the model proved to be time-intensive and demanded a substantial volume of data.

A deep neural network, with its layered structure and various activation functions, learns to recognise patterns at different levels of complexity within the ECG signals. Specifically, the CNN stands out for its ability to extract and identify features within ECG signals, making it highly effective for tasks such as diagnosing cardiac conditions and predicting patient outcomes based on ECG data. The CNN architecture has been devised to diagnose various CVD applications, including arrhythmia conditions [22, 23, 24, 25], atrial fibrillation (AF) [26], and CAD [9, 10, 21, 27]. The performance evaluation of the CNN model relies on its capacity to accurately process input signals and produce the intended prediction. This evaluation focuses on how effectively the CNN interprets and manages the provided ECG signals to classify potential classes. An 11-layer CNN model, combined with Discrete Wavelet Transform (DWT), achieved an accuracy of 94.95% in 2-second segments and 95.11% in 5-second segments. The DWT with the Daubechies 6 (db6) mother wavelet was employed on the ECG signals to mitigate noise and baseline wander [21]. The CNN model possesses the capability to extract features from ECG signals, but its efficacy depends on the quality of the ECG data. When data is corrupted by noise and artefacts, it compromises the model's learning capacity. Thus, preprocessing methodologies, including DWT [21, 28], various entropy computations [29], and the Fourier transform [30], are applied to enhance the quality of the signal before its incorporation into the CNN model.

Due to a significant shortage of available CAD data, a relatively small group of researchers have conducted their work on CAD diagnosis [10, 21, 31]. Even among these works, many studies have focused on detecting arrhythmia [24, 25], congestive heart failure [32], AF [26] and MI [33].

A recent study proposed a CNN–LSTM–SE architecture for classifying heart failure severity using lead II ECG signals from the MIMIC III database [34]. While the focus was on heart failure, it demonstrates the effectiveness of applying deep learning methods to ECG data from MIMIC III. Other recent studies have also explored classification tasks using MIMIC III, including a multimodal contrastive learning approach that combines ECG signals with clinical text for arrhythmia detection [35], and a traditional k-NN method using handcrafted ECG features for atrial fibrillation identification [36]. These studies highlight the potential of MIMIC III for ECG-based classification. Yet, despite its widespread prevalence, very limited attention has been given to CAD [37]. The main focus of many existing studies relies on these heart diseases, primarily due to the availability of datasets as previously mentioned. Furthermore, these diseases are easily distinguishable into potential classes due to their specific and distinctive biomarkers. On the contrary, CAD, which lacks certain biomarkers, presents more formidable challenges. Recent deep learning approaches to CAD detection have primarily focused on deeper CNN architectures, often overlooking critical factors such as signal quality issues and real-time applicability [38]. This paper addresses these limitations by proposing a streamlined 1D-CNN architecture, designed for CAD detection. By targeting this underexplored area, the study contributes to closing a notable gap in the current literature.

In this study, we aim to design a specific deep learning-based model for accurate coronary artery disease classification. The summary of the contributions is as follows:

- A smart feature engineering is proposed to remove unwanted and noisy ECG segments prior to model training, improving data quality and overall model reliability.
- A novel and streamlined 1D-CNN architecture is developed, integrated with the FE module for CAD diagnosis. This integration enhances noise tolerance, improves generalisability to unseen data, and supports efficient deployment in real-time settings.
- The MIMIC III dataset is prioritised for CAD diagnosis, with extensive preprocessing conducted to address the

complexity and noise inherent in its ECG signals.
- To verify the effectiveness of our proposed model, we conduct a comparative analysis of classical machine learning models alongside existing CNN-based models on well-established datasets.
- A one-class evaluation is conducted to assess the model's ability to distinguish CAD from non-CAD cases, reflecting realistic screening scenarios in clinical practice.
- A cost-effective and time-efficient diagnostic pipeline is designed to support scalable CAD screening, particularly in clinical and resource-constrained settings.

Moreover, while much of the existing literature focuses on arrhythmia classification using ECG signals, the proposed model is specifically developed for CAD detection, which is a clinically significant yet relatively underexplored application. Our primary aim is to develop a cost-effective and time-efficient diagnostic tool suitable for use in real-world healthcare environments. To facilitate clinical use, the proposed model is designed for fully automated operation, enabling rapid and accurate CAD diagnosis to support improved the standard of patient care. Additionally, the model's robustness is evaluated under varying conditions by comparing its performance on data with and without feature engineering techniques.

II. MATERIALS AND METHODS

The proposed method comprises three key phases: data preparation, feature engineering, and developing a deep learning model. We aim to design and implement a model to classify CAD using ECG signals, based on a comprehensive series of experiments. Subsequent sections will provide detailed explanations of each step.

A. DATA PREPARATION

The primary source for training and testing ECG data is derived from the MIMIC III and Fantasia databases, accessible on the Physionet website [39, 40]. Around 2,840 patients, comprising roughly 7.1% of the total hospital admissions, have been identified within the MIMIC database as individuals diagnosed with coronary atherosclerosis in the native coronary artery. On the other hand, the Fantasia database is characterised by a cohort consisting of 40 individuals, with an equal distribution of 20 young and 20 adult patients. The acquisition of ECG signals is facilitated by employing ECG sensors. The ECG electrodes are strategically positioned on the patient's body, enabling the sensors to accurately capture the activity of the heart. The ECG signal consists of the P wave, representing atrial depolarisation; the QRS complex, indicating ventricular depolarisation and contraction; and the T wave, demonstrating ventricular repolarisation and relaxation. ST depression indicates significant coronary artery lesions, highlighting a critical need for an early invasive treatment. Moreover, ST elevation displays a complete blockage of the artery, indicating CAD, MI, or a heart attack. To create a balanced dataset for each class, forty patients were meticulously selected from each respective database and partitioned into 1-second segments of ECG data, resulting in approximately 500,000 seconds. Maintaining class balance is crucial for minimising model bias and ensuring reliable detection of minority class instances. In the presence of class imbalance, the model may exhibit reduced sensitivity to CAD cases, potentially compromising diagnostic performance. The segmentation process facilitates a thorough analysis of the dynamic changes and patterns within ECG signals over short time frames. This approach has been widely employed in most of the previous works to ensure consistency in the ECG signal [10, 41, 42]. Hence, in our study, the ECG data was segmented into small segments to maintain consistency. The aim is to guarantee that each segment contains a complete ECG cycle, without relying on QRS detection [42]. These segments will be employed to apply FE techniques, which include Sample Entropy and Standard Normalisation, to systematically eliminate irrelevant and noisy ECG data that may potentially affect the predictive accuracy of the model (see next section).

B. FEATURE ENGINEERING

ECG signals are fundamental clinical tools for diagnosing cardiac diseases. However, the integrity of these signals is frequently compromised by prevailing challenges, including baseline drift, muscular interferences, powerline artifacts, and electrode motion disruptions. These challenges have a significant negative impact on the quality of ECG signals, rendering specific segments of the data inadequate for precise diagnosis [21, 43]. Furthermore, they impede individuals' awareness of their health status.

FE plays a significant role as it assists in removing missing or inconsistent ECG data resulting from human and equipment errors. It aids in transforming raw ECG data into informative features, which enable the model to better capture underlying patterns and improve its predictive accuracy. Sample entropy serves as a metric utilised to assess the quality of time series data. Its efficacy in mitigating noisy ECG channels has been demonstrated in previous research [44]. Furthermore, standard normalisation is employed to eliminate flat time series data and to mitigate any potential data that could impact accuracy. The computation of sample entropy is presented as follows in equation (1).

$$SampEn = -\ln\left(\frac{\sum_{i=1}^{N-m} Q_i^m(r)}{\sum_{i=1}^{N-m+1} P_i^{m+1}(r)}\right) \tag{1}$$

where $SampEn$ indicates the quality of the ECG signals. N represents the number of samples within each 1-second ECG segment. m refers to the embedded dimension, which represents the length of consecutive samples or data points analysed together. $Q_i^m(r)$ quantifies the instances of vector pairs of dimension m whose mutual distance falls below a predefined threshold r, suggesting a degree of similarity or regularity within the signal. $P_i^{m+1}(r)$ quantifies the number of vector pairs of dimension $m+1$ that are similar within

a predefined threshold level r, thereby extending the comparison to sequences of increased length. A value of r =0.1 was employed in this study, consistent with prior literature suggesting that values within the range of 0.1 to 0.25 are effective for preserving the quality of ECG signals [45].

Standardisation is then applied to minimise flat regions and noisy artifacts in the ECG signals, thereby improving the representation of key morphological features. The computation of standard normalisation is detailed in equation (2).

$$\sigma = \sqrt{\frac{1}{N-1}\sum_{i=1}^{N}(x_i - \bar{x})^2} \tag{2}$$

where σ also indicates the quality of the ECG signals, N is the number of signals, $\bar{x}$ is the average of a given signal, and x_i is the signal value at the i^{th} position.

To summarise, FE using *SampEn* and standard normalisation was employed to remove ECG segments that exhibited flat lines or an absence of clear clinical features. These artefacts were caused by baseline wander, motion noise or poor electrode contact during signal acquisition. Although DL-based models perform automatic feature extraction, FE was applied to improve signal quality by removing low-information ECG segments. This step ensures that the input retains clinically meaningful waveform components, thereby enhancing model robustness and generalisability.

Importantly, FE is applied during both training and prediction to ensure that only clinically relevant and high-quality ECG segments are used. This consistency improves the model's robustness and generalisability in real-world clinical applications. In clinical use, it also enables the system to focus on meaningful ECG input and reduces the risk of misclassification caused by noise or incomplete signals.

Figure 1 presents a comparison of exemplary ECG signals, showcasing examples of both high-quality and poor-quality signals. FE is applied to the 1-second ECG segments generated in the previous step. The threshold r is set at 0.1, which is used to determine the quality of the signal. Signals with a value less than r are classified as high-quality signals. The segments in which ECG signals fail to meet the specified threshold r are excluded. In Figure 1(a), an exemplary ECG signal demonstrating high quality is depicted. This signal displays distinct ECG features, such as well-defined cycles containing QRS complexes and other waveforms. Conversely, Figure 1(b) illustrates an exemplary ECG signal demonstrating poor quality. This signal is characterised by the absence of clear ECG features, and it contains noise patterns indicative of potential recording or signal acquisition issues. Therefore, it is crucial to ensure the reliability of ECG signals in subsequent processes, as it helps mitigate the risk of generating inaccurate predictive outcomes.

Figure 2 illustrates a comparison of the quality of ECG signals after applying standard normalisation to remove remaining noise and flatness. A signal is retained as high quality if its standard deviation exceeds the threshold r. Conversely, signals with the standard deviation below the threshold r are

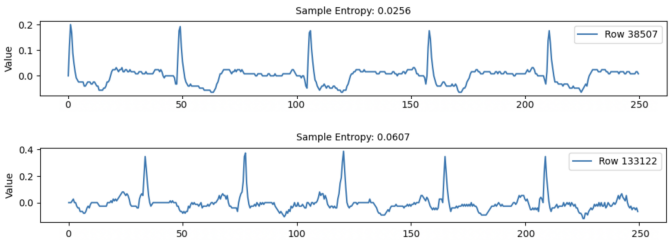

((a)) Exemplary ECG Signal Demonstrating High Quality

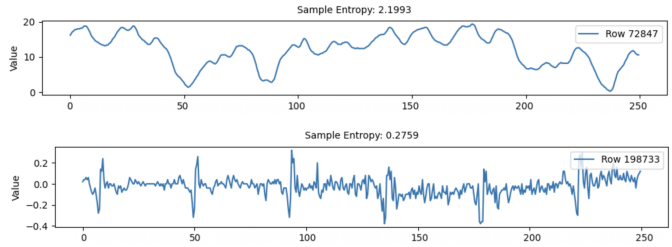

((b)) Exemplary ECG Signal Demonstrating Poor Quality

FIGURE 1: Signal Quality Evaluation: ECG Signals with sample entropy below threshold (r = 0.1) retained for further processing

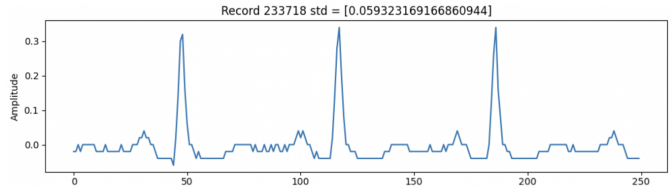

((a)) Poor-Quality ECG Signal with flat line

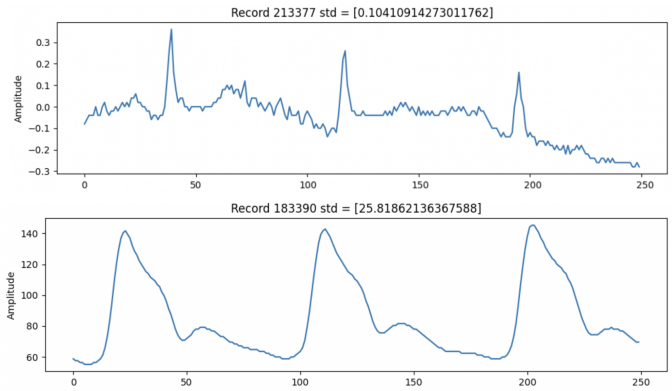

((b)) Good-Quality ECG Signal without flat line

FIGURE 2: Signal Quality Evaluation: ECG Signals with standard normalisation above threshold (r = 0.1) retained for further processing

excluded. This FE technique is employed to eliminate any flatness present in the signal, thereby reducing the risk of low predictive accuracy. It serves as an optional approach to ensure signal cleanliness, aimed at preserving signal integrity and thereby enhancing the model's capacity for pattern recognition. After applying the FE techniques, the retained ECG signal is then inputted into the proposed model for the classification of CAD and non-CAD cases.

C. CNN MODEL

A CNN model consisting of four convolutional layers, a max-pooling layer, four dropout layers, a flattened layer, and a fully connected dense layer was designed. ECG signals are taken as input to the first layer of the convolutional layer. The convolutional layer was used to learn and extract patterns of two possible classes (CAD and non-CAD). The output of the convolutional layer is calculated as:

$$y(n) = \begin{cases} \sum_{i=0}^{k} x(n+i)h(i), & \text{if } n = 0 \\ \sum_{i=0}^{k} x(n+i+(s-1))h(i), & \text{otherwise} \end{cases} \quad (3)$$

where $y(n)$ represents the output signal at position n within the convolutional layer, $x(n)$ denotes the ECG input signal, and $h(i)$ signifies the convolutional kernel—a collection of learnable weights that the CNN acquires during training for feature extraction from the input signal $x(n)$. The parameter k corresponds to the size of the convolutional kernel, determining the receptive field, which defines the spatial area over which the filter operates on the input signal. s represents the stride length, indicating how the convolutional kernel moves through the ECG signal. s is set to 1 by default, indicating that the kernel progresses through the input signal with each step equivalent to the size of one ECG sample.

Figure 3 illustrates that the initial convolutional layer consists of 512 filters with a kernel size of 32, while the subsequent layers consist of 256 filters, each with the same kernel size. The Rectified Linear Unit (ReLU) activation function was used in the convolutional layers to introduce non-linearity into the model, thereby aiding in the comprehension of intricate patterns within the ECG signal. Three dropout layers with a rate of 0.2 were added after the convolutional layers to prevent overfitting. The max pooling layer with a pool size of 128 was then applied to reduce the spatial size of the feature maps and improve generalisation by selecting the maximum value within a window size. The flattened output was then passed to a fully connected layer, consisting of 128 neurons and employing the ReLU activation function. To further prevent overfitting, an additional dropout layer with a rate of 0.5 was incorporated before the final output layer. The final layer comprises two neurons and utilises softmax activation, enabling the model to classify input data into one of two potential classes, thereby representing the probabilities of the input belonging to each class.

A binary cross-entropy loss function is used for CAD and non-CAD classification due to its ability to handle binary classification tasks as shown in (4).

TABLE 1: Hyperparameters used for model training

Hyperparameter	Value
Learning Rate	0.0001
Batch Size	32
Number of Epochs	50
Optimiser	Adam
Loss Function	Binary Cross-Entropy
Hidden Layer Activation	ReLu
Output Layer Activation	Softmax

$$\text{BinaryCrossEn} = -\frac{1}{N}\sum_{i=1}^{N}\left(y_i \log(p_i) + (1-y_i)\log(1-p_i)\right) \quad (4)$$

where N is the number of samples in the corresponding ECG segment. y_i is the true label for ECG signals i, where $y_i \in \{0, 1\}$. $y_i = 0$ represents a non-CAD case, indicating the absence of CAD features in the ECG signal i. Conversely, $y_i = 1$ exhibits a CAD case, representing the existence of relevant CAD features in the ECG signal i. p_i is a predicted probability that ECG signal i belong to class 1. It facilitates the model in determining its predictive certainty, thereby refining its prediction to achieve better alignment with the true labels.

The hyperparameters used during model training, including learning rate, batch size, and number of epochs, are summarised in Table 1.

III. EXPERIMENTAL RESULTS

In this section, the performance of the proposed model is evaluated, including classification accuracy and comparative analysis with other models.

A. EXPERIMENTS

As outlined in Section II-A, forty patients were deliberately sampled from both the MIMIC and Fantasia databases in identical proportions. Subsequently, the data was partitioned into 1-second segments (each with $N = 250$ samples) to enhance accuracy and focus on temporal aspects. After segmenting the ECG data into 1-second segments and implementing feature engineering techniques, two distinct subsets of data are generated for the experiments: D_1 and D_2. The first subset (D_1) comprises 100 CAD samples and 100 NON-CAD samples, with each sample having a length of 1 second. To assess the model's performance robustly, we employed k-fold cross-validation on D_1 by partitioning it into 10 folds. In each iteration, 70% of the folds were used for training, and the remaining 30% for validation. The partitioning method is extensively utilised due to its dual capacity to provide substantial training data and allocate sufficient resources for assessing the model's ability to generalise. Moreover, subset D_2, containing an equivalent number of samples as D_1, was used exclusively for testing to assess the model's ability to generalise to unseen data.

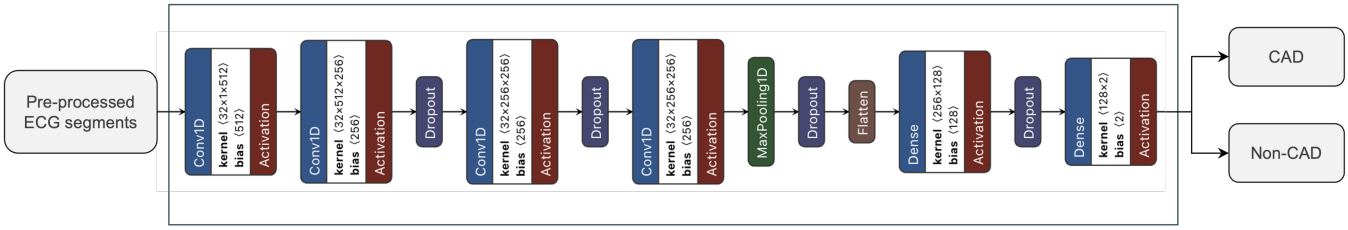

FIGURE 3: The proposed model architecture.

To evaluate the model, performance metrics including Accuracy, Error Rate, Precision (*Ppr*), Sensitivity (*Sen*), Specificity (*Spr*), and F1 Score (*F1*) were used to measure the performance of the classification model as shown in (5)-(10).

$$Accuracy = \frac{TP + TN}{TP + TN + FP + FN} \tag{5}$$

$$Errorrate = 1 - Accuracy \tag{6}$$

$$Ppr = \frac{TP}{TP + FP} \tag{7}$$

$$Sen = \frac{TP}{TP + FN} \tag{8}$$

$$Spr = \frac{TN}{TN + FP} \tag{9}$$

$$F_1 = \frac{2 \times \text{Sen} \times \text{Ppr}}{\text{Sen} + \text{Ppr}} \tag{10}$$

where true positives (TP) are the CAD cases that the model correctly identifies as CAD, true negatives (TN) are the non-CAD cases correctly identified as non-CAD, false positives (FP) are the non-CAD cases mistakenly identified as CAD, and false negatives (FN) are the CAD cases mistakenly identified as non-CAD.

B. RESULTS AND DISCUSSION

To assess the impact of FE, we conducted ablation experiments. Models trained without FE exhibited lower accuracy and generalisation, particularly on unseen data (D_2), confirming the role of FE in reducing irrelevant and noisy components. Table 2 demonstrates the investigation of the model's performance with and without FE, aimed at studying its impact on the proposed model. The effectiveness of the proposed model is notably high, achieving an accuracy of 99.3% on the training set and 98.5% on the testing (D_1). Moreover, it showcased robust performance on unseen data from D_2, achieving a noteworthy accuracy of 99.0%. In contrast, the proposed model yielded lower accuracy when feature engineering was not applied to both datasets, with D_2 exhibiting an accuracy of 87.0%. To summarise this investigation, it proves that applying FE significantly improves the model's ability to accurately classify instances of CAD and non-CAD cases. Particularly, FE facilitates the model in eliminating irrelevant data, thereby mitigating model potential issues, leading to higher accuracy rates.

TABLE 2: Accuracy Comparison with and without FE on Datasets D_1 and D_2.

Model	D_1		D_2
	Train (%)	Test (%)	Unseen (%)
Without FE	85.1	87.9	87.0
With FE	99.3	98.5	99.0

** FE is a Feature Engineering*

Table 3(a) presents the performance of classical machine learning models, while Table 3(b) presents the performance results for deep learning models on D_1 and D_2, with and without FE applied. In the absence of FE implementation, the proposed model performed admirably on D_1, achieving 85.1% accuracy on the training set and 87.9% on the testing set. It also achieved the highest accuracy on previously unseen data from D_2, reaching 87.0%. Although kNN reported a higher training accuracy of 96.3% on D_1, it demonstrated poor generalisability, with its accuracy dropping to 49.0% on D_2. SVM and K-means also showed reduced accuracy without FE; SVM achieved 65.2% on the D_1 test set and 63.0% on D_2, while K-means attained 59.1% and 60.0%, respectively. The application of FE notably improved the performance of all classical models, underscoring their reliance on engineered features for effective classification.

In comparison to the classical machine learning methods, deep learning models exhibited stronger generalisation across both datasets. Without FE, the LSTM model achieved a test accuracy of 78.3% on D_1 and 77.5% on D_2, while the CNN-LSTM model yielded a comparable accuracy of 79.0% on D_2. With FE, these results improved further, with the LSTM reaching 90.0% and CNN-LSTM achieving 89.0% on D_2, demonstrating the ability of temporal models to learn sequential dependencies directly from raw ECG signals.

Among all classical machine learning and deep learning models, the proposed model demonstrates exceptional performance in binary classification on both datasets when FE is applied, achieving accuracy rates of 99.3% on the training set and 98.5% on the testing set of D_1. Additionally, the trained model demonstrated strong performance by achieving a classification accuracy of 98.5% on unseen data from D_2. SVM and kNN demonstrated strong performance on D_1, obtaining accuracy rates of 95.5% and 96.9%, respectively. However,

TABLE 3: Performance comparison of classical machine learning and deep learning algorithms on D_1 and D_2, with and without FE applied.

(a) Classical Machine Learning Models

Model	Without FE			With FE		
	D_1		D_2	D_1		D_2
	Train (%)	Test (%)	Unseen (%)	Train (%)	Test (%)	Unseen (%)
SVM	64.2	65.2	63.0	95.5	96.1	96.4
K-means	60.4	59.1	60.0	86.6	93.9	89.0
kNN	96.3	82.5	43.5	96.9	97.5	49.0

(b) Deep Learning Models

Model	Without FE			With FE		
	D_1		D_2	D_1		D_2
	Train (%)	Test (%)	Unseen (%)	Train (%)	Test (%)	Unseen (%)
LSTM [46]	76.2	78.3	77.5	92.6	86.7	90.0
CNN-LSTM [46]	79.3	78.3	79.0	92.9	86.7	89.0
Proposed Model	85.1	87.9	87.0	99.3	98.5	99.0

kNN struggled to generalise to unseen data from D_2, while SVM maintained its effectiveness, achieving an accuracy of 96.4%. The performance of K-means is noteworthy that its performance appears relatively subpar when evaluated on the training data D_1. However, it displays a notable improvement in classifying unseen data D_2, surpassing the performance of the kNN. The investigation reveals that the proposed model outperformed in the application of CAD, particularly in cases where no certain biomarker represented its signal. This underscores a significant aspect of classical machine learning models, as it heavily relies on the extraction of precise features for the model to effectively capture and learn patterns. Moreover, machine learning is adept at handling small datasets effectively. Nevertheless, as our dataset scales up considerably, deep learning emerges as a more appropriate approach owing to its capability to manage intricate and expansive data structures proficiently. As evidenced by the outcomes of this investigation, it validates and clarifies our reasoning for selecting deep learning over classical machine learning algorithms in our application.

Figure 4(a) illustrates the performance metrics for CAD detection in D_1 and provides valuable insights into the model's effectiveness. With an accuracy of 99.3%, the model demonstrates its capability to correctly classify all CAD and non-CAD instances, indicating solid overall performance with an error rate of 0.7%. The *Ppr* is 98.5%, indicating that nearly all positive predictions were correct. Similarly, *Sen* was observed to be 98.5%, suggesting that the model accurately identified the majority of actual CAD cases. Additionally, a *Spr* of 100% highlights the model's proficiency in accurately identifying negative cases, implying a satisfactory ability to distinguish non-CAD instances. Moreover, the *F1 score*, a metric that balances precision and recall, was calculated at 99.01%, indicating a strong overall performance of the model in accurately classifying both CAD and non-CAD cases on the training data.

Figure 4(b) shows an overall accuracy of about 98.5% on testing data. The model correctly predicted 34 instances of Class 1. This indicates a strong ability of the model to identify CAD cases. Similarly, the model correctly predicted 31 instances of class 0, which demonstrates the model's effectiveness in identifying non-CAD cases. There was 1 instance where the model incorrectly predicted class 1 as class 0. This error indicates a slight issue with the model's sensitivity to identifying CAD cases.

Figure 4(c) illustrates that the model has a high degree of proficiency, achieving an exceptional accuracy rate of 99.0%. The model accurately predicted CAD for 98 instances and non-CAD for 100 instances. Additionally, there were 2 instances where the model incorrectly predicted non-CAD as CAD cases, but there were no instances where CAD was incorrectly predicted as non-CAD. Notably, the *Ppr* for class 1 demonstrates a commendable figure of 98%, indicating the model's accuracy in identifying CAD cases. Additionally, the *Sen* for class 1 is outstanding, signifying that the model successfully captures all instances of class 1 present in the dataset D_2. Furthermore, the *F1 score*, which combines precision and recall into a single metric, is approximately 98.99% for

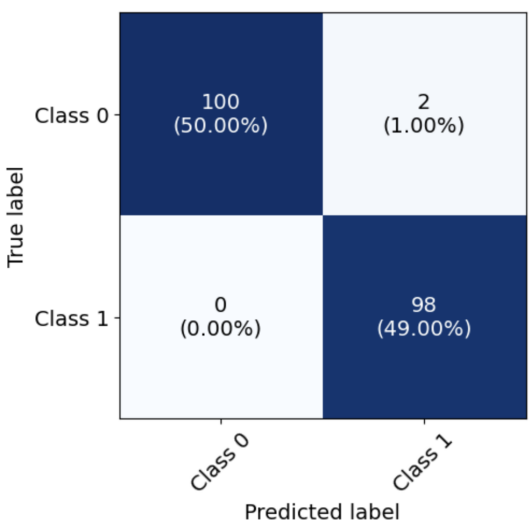

(a) on Training Data D_1

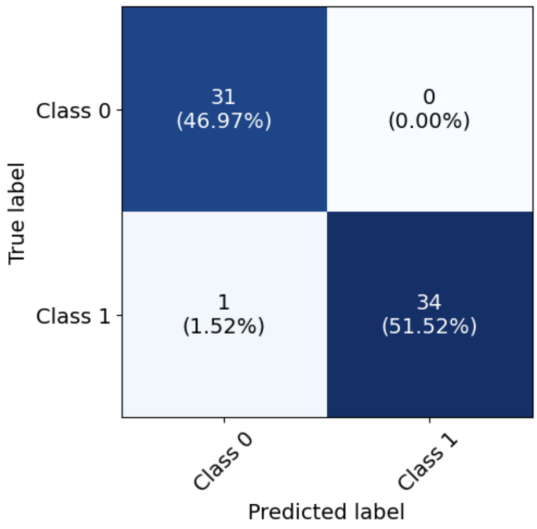

(b) on Test Data D_1

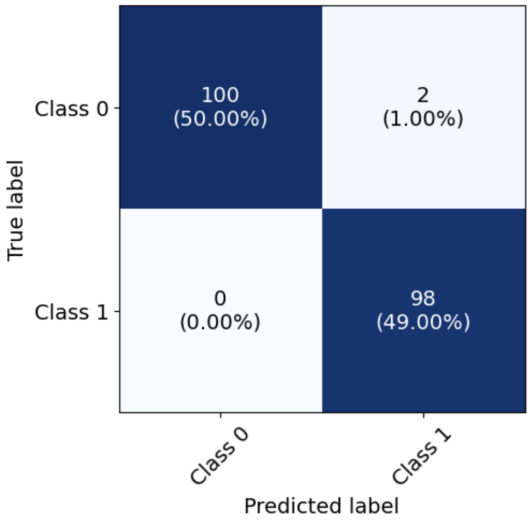

(c) on Test Data D_2

FIGURE 4: Confusion Matrix Analysis on D_1 and D_2

class 1, suggesting a well-balanced performance in this binary classification.

Figure 5 demonstrates the confusion matrices used to evaluate the accuracy of our proposed model in a one-class classification case. The model was trained on a balanced dataset comprising both CAD and NON-CAD samples. For evaluation purposes, we tested the classifier on two distinct datasets: one containing only CAD samples, with no NON-CAD samples, and the other containing only NON-CAD samples. This approach allows for a clear assessment of the model's capability to accurately identify each class in isolation. Figure 5(a) demonstrates that the classifier accurately is 99%, with only one sample misclassified as NON-CAD. Similarly, Figure 5(b) illustrates that the classifier correctly identified 98% of NON-CAD samples correctly. With a true positive rate of 99% for CAD samples and a true negative rate of 98% for NON-CAD samples, the model exhibits robust performance metrics. The notably low false negative rate in CAD detection is especially crucial, as it ensures that nearly all patients with CAD are accurately identified. Similarly, the low false positive rate in NON-CAD detection helps prevent misdiagnoses.

Figure 6 exhibits the performance comparison of classical machine learning algorithms and our proposed model, evaluated on CAD classification. The k-means model, depicted in blue, has an Area Under the Curve (AUC) of 0.10, showing weak performance due to its proximity to the random guess line, suggesting that the model's performance is not much better than random chance. The SVM, depicted in orange, and the kNN, shown in green, both exhibit a high level of discriminative ability with an AUC of 0.98. The Proposed model is represented by the red line and has the highest AUC of 0.99,

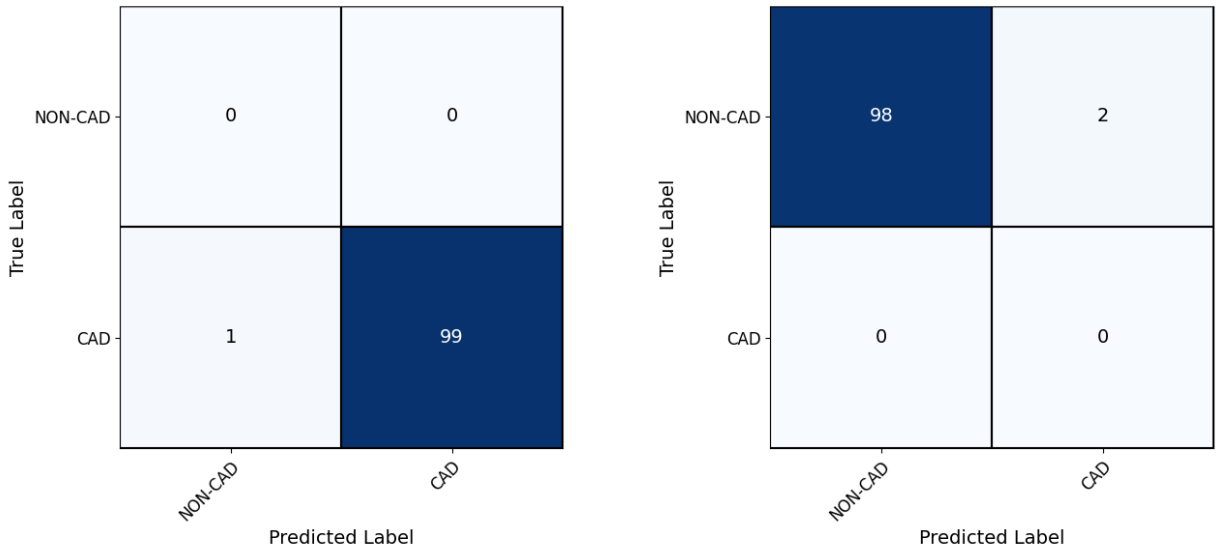

(a) on 100 CAD ECG samples

(b) on 100 NON-CAD ECG samples

FIGURE 5: Confusion Matrix: One-Class Testing Performance

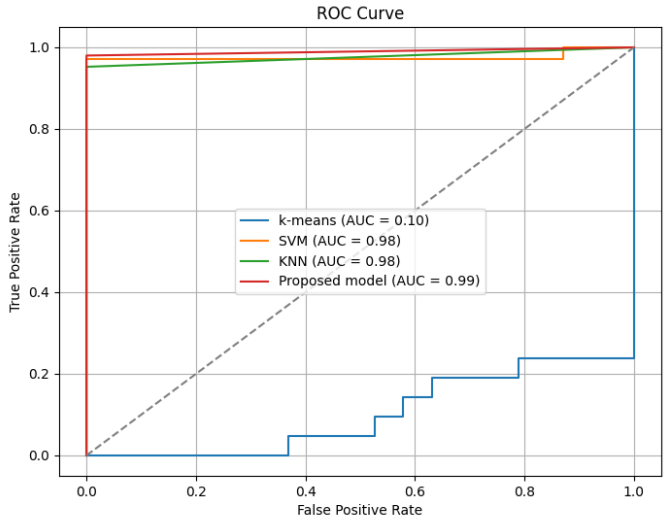

FIGURE 6: Analysis of Classifier Efficacy Through ROC Curve Metrics

which suggests that it has the best performance among the models presented. The SVM and kNN models exhibit strong performance, as evidenced by their high AUC values, indicating their proficiency in effectively discriminating between CAD and non-CAD cases. On the contrary, the proposed model exhibits slight enhancements when compared to SVM and kNN. This improvement stems from the CNN's ability to automatically extract relevant features from the dataset, identifying complex patterns and relationships that SVM and kNN may overlook. Consequently, the proposed model achieves a slightly higher level of discrimination, resulting in its slightly improved performance. This outcome is anticipated, as k-means clustering operates by grouping data points according to their similarity, rather than assigning them to predetermined categories, which is essential in classification tasks. As a result, among the other models, k-means exhibits the lowest performance in classifying CAD and non-CAD cases.

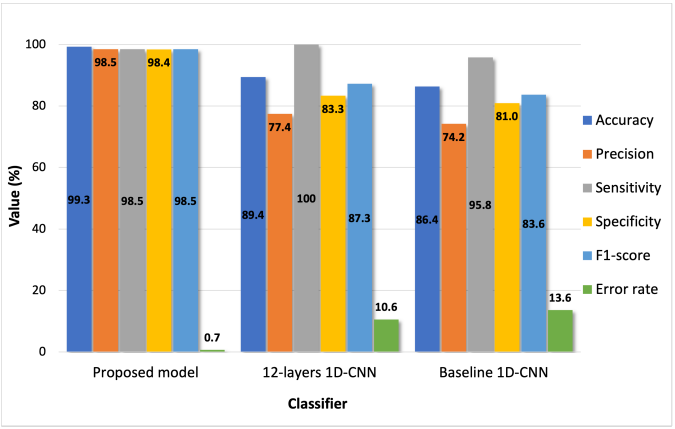

FIGURE 7: Comparison among Existing CNN Models with Feature Engineering Module

Figure 7 illustrates the application of existing CNN models to our datasets. Following the findings presented by [47], which demonstrated a 93.33% accuracy rate for AF diagnosis using a 12-layer 1D-CNN architecture, our study aimed to expand upon this research. Employing the 12-layer CNN model on our datasets resulted in an accuracy of 89.4%. Furthermore, a baseline 1D-CNN model is employed for diagnosing cases of CAD, achieving an accuracy of 87% as reported

in [9]. In our study, upon implementing this model to our datasets, we achieved an accuracy of 86.4%. The proposed model exhibits strong predictive capabilities, achieving the highest accuracy of 99.3% compared to the other models. It also boasts a precision of 98.5%, sensitivity of 98.5%, specificity of 98.4%, and an F1 score of 98.5%. Impressively, it maintains a notably low error rate of 0.7%. Comparatively, the 12-layer 1D-CNN model also demonstrates strong performance, although with a significantly higher error rate of 10.6% compared to the proposed model. Furthermore, the 12-layer 1D-CNN appears to perform better compared to the baseline model. The baseline 1D-CNN model, on the other hand, falls short with a higher error rate of 13.6%, suggesting its inferior performance in comparison to the other two models. Therefore, the observed results indicate that FE has a notable influence on the model's capacity to accurately distinguish between features associated with CAD and non-CAD cases. The FE appears to improve the model's ability and its overall performance in CAD diagnosis.

Several recent studies have applied machine learning and deep learning techniques to the detection of CAD [21, 28, 37]. For instance, hybrid CNN-LSTM models have been used to classify ECG signals, while traditional approaches based on handcrafted features have also shown promise in early diagnosis [9]. These benchmarking studies reflect the growing interest in automated CAD detection. In contrast to existing methods, the proposed model combines feature engineering with a compact CNN architecture, achieving strong classification performance alongside improved computational efficiency. This design enables practical deployment in both clinical and portable settings. By filtering low-quality ECG segments prior to classification, the method enhances signal relevance while preserving key diagnostic features. Furthermore, the reduced model complexity supports real-time application, representing a meaningful advancement over previous CNN-based CAD approaches.

TABLE 4: Model inference time comparison for CAD classification

Model	Avg. Inference Time per Subject (ms)
SVM	0.051
K-Means	0.132
KNN	1.142
LSTM	28.746
CNN-LSTM	22.194
Proposed model	18.731

Alongside classification accuracy, computational efficiency is an important factor in ensuring a model is suitable for real-world use, particularly in clinical environments where time and resources may be limited. As shown in Table 4, we compared the average inference time per subject across a range of traditional and deep learning models. While traditional methods offer very fast inference times, they typically underperform in classification accuracy compared to deep learning approaches, as highlighted in Table 3. The proposed model completes inference in 18.731 ms, which is faster than more complex models such as LSTM at 28.746 ms and CNN-LSTM at 22.194 ms. These results suggest that the model is not only accurate but also efficient enough for real-time use, including applications in bedside monitoring or portable ECG devices where quick and reliable decisions are essential.

IV. DISCUSSION AND FUTURE DIRECTIONS

Table 5 presents a comparison of recent ECG-based classification models evaluated on the MIMIC III dataset. While previous studies have addressed various cardiovascular conditions such as arrhythmia [35], heart failure [34, **?**], and atrial fibrillation [36], there is a notable absence of research focusing specifically on the detection of CAD using MIMIC III ECG signals. This gap highlights the limited exploration of CAD in large publicly available clinical ECG datasets, despite its high prevalence and clinical importance. To address this, the proposed 1D-CNN model is developed and evaluated for CAD detection, achieving a competitive accuracy of 99.0% and demonstrating the potential for automated CAD classification using MIMIC III ECG data.

Future studies should consider evaluating model performance across diverse patient subgroups, including those defined by age, sex, and ethnicity, to enhance both representativeness and clinical applicability of the proposed approach. Although this study focuses on binary classification of CAD, examining the model's performance across different CAD subtypes could provide deeper insight into its ability to distinguish between them. Extending the model to support multi-class classification of these CAD subtypes would be a valuable step towards enhancing its clinical usefulness. In future work, the approach could also be adapted to detect other forms of heart disease, such as arrhythmias or heart failure. Further studies could investigate alternative segmentation techniques that offer significant insights into ECG CAD signals. Furthermore, focusing on reducing complexity while maintaining accuracy could enhance real-time health monitoring capabilities for practical settings. As a result, the model will be optimised and implemented on a practical sensing-and-processing device such as STM32F469I-DISCO. With its compact structure and ability to handle noisy signals, the proposed model is well-suited for use as a pre-screening tool in clinical settings, where it can assist with the review of ECG signals before cardiologist assessment.

V. CONCLUSION

Our study developed a CNN model to classify potential cases of CAD using ECG signals. By utilising data sourced from PhysioNet, it was revealed that the CNN model could independently classify binary classes. However, we observed a significant improvement in its performance when it was preceded by feature engineering and pre-processing of the ECG data. The performance of the proposed model exceeded that of other CNN models investigated in our study, highlighting the importance of feature engineering in increasing the model's ability to learn and make accurate predictions. Furthermore, our examination of three distinct classical machine

TABLE 5: Comparison of ECG-Based Classification Methods on MIMIC-III Dataset

Paper (Year)	Disease/Task	Methods	Data Split	Accuracy (%)
Vanitha et al., 2025 [35]	Arrhythmia	Multi modal Contrastive Learning	Not specified	97.8
Zhang et al., 2024 [34]	Heart Failure	CNN-LSTM-SE	70% train, 10% val, 20% test	99.1
Bashar et al., 2020 [36]	Atrial Fibrillation	k-NN	10-fold + 2 independent test sets	99.3
Proposed Model	CAD	1D-CNN	10-fold + 2 independent test sets	99.0

learning algorithms revealed that the CNN model surpassed these methods in predicting CAD. These findings indicate the significance of feature engineering in enhancing the CNN model performance, highlighting the CNN model's superiority over conventional methods in CAD diagnosis.

REFERENCES

[1] Who.int., "Cardiovascular diseases." https://www.who.int/health-topics/cardiovascular-diseases, 2019.

[2] C. D. Mathers and D. Loncar, "Projections of global mortality and burden of disease from 2002 to 2030," *PLoS medicine*, vol. 3, no. 11, p. e442, 2006.

[3] M. J. Pencina, A. M. Navar, D. Wojdyla, R. J. Sanchez, I. Khan, J. Elassal, R. B. D'Agostino Sr, E. D. Peterson, and A. D. Sniderman, "Quantifying importance of major risk factors for coronary heart disease," *Circulation*, vol. 139, no. 13, pp. 1603–1611, 2019.

[4] R. Hajar, "Risk factors for coronary artery disease: historical perspectives," *Heart views: the official journal of the Gulf Heart Association*, vol. 18, no. 3, p. 109, 2017.

[5] A. D. Dolatabadi, S. E. Z. Khadem, and B. M. Asl, "Automated diagnosis of coronary artery disease (cad) patients using optimized svm," *Computer methods and programs in biomedicine*, vol. 138, pp. 117–126, 2017.

[6] W. Zhu, X. Chen, Y. Wang, and L. Wang, "Arrhythmia recognition and classification using ecg morphology and segment feature analysis," *IEEE/ACM Transactions on Computational Biology and Bioinformatics*, vol. 16, no. 1, pp. 131–138, 2019.

[7] M. U. Khan, S. Aziz, S. Z. Hassan Naqvi, and A. Rehman, "Classification of coronary artery diseases using electrocardiogram signals," in *2020 International Conference on Emerging Trends in Smart Technologies (ICETST)*, pp. 1–5, 2020.

[8] M. Merino, I. M. Gomez, and A. J. Molina, "Envelopment filter and k-means for the detection of qrs waveforms in electrocardiogram," *Medical engineering & physics*, vol. 37, no. 6, pp. 605–609, 2015.

[9] R. Banerjee, A. Ghose, and K. Muthana Mandana, "A hybrid cnn-lstm architecture for detection of coronary artery disease from ecg," in *2020 International Joint Conference on Neural Networks (IJCNN)*, pp. 1–8, 2020.

[10] J. H. Tan, Y. Hagiwara, W. Pang, I. Lim, S. L. Oh, M. Adam, R. S. Tan, M. Chen, and U. R. Acharya, "Application of stacked convolutional and long short-term memory network for accurate identification of cad ecg signals," *Computers in Biology and Medicine*, vol. 94, pp. 19–26, 2018.

[11] S. Singh, S. K. Pandey, U. Pawar, and R. R. Janghel, "Classification of ecg arrhythmia using recurrent neural networks," *Procedia computer science*, vol. 132, pp. 1290–1297, 2018.

[12] Y. Guan, Y. An, J. Xu, N. Liu, and J. Wang, "Ha-resnet: Residual neural network with hidden attention for ecg arrhythmia detection using two-dimensional signal," *IEEE/ACM Transactions on Computational Biology and Bioinformatics*, vol. 20, no. 6, pp. 3389–3398, 2023.

[13] S. Yang, C. Lian, Z. Zeng, B. Xu, J. Zang, and Z. Zhang, "A multi-view multi-scale neural network for multi-label ecg classification," *IEEE Transactions on Emerging Topics in Computational Intelligence*, vol. 7, no. 3, pp. 648–660, 2023.

[14] A. Ballas and C. Diou, "Towards domain generalization for ecg and eeg classification: Algorithms and benchmarks," *IEEE Transactions on Emerging Topics in Computational Intelligence*, vol. 8, no. 1, pp. 44–54, 2024.

[15] S. Nurmaini, A. Darmawahyuni, A. N. Sakti Mukti, M. N. Rachmatullah, F. Firdaus, and B. Tutuko, "Deep learning-based stacked denoising and autoencoder for ecg heartbeat classification," *Electronics*, vol. 9, no. 1, 2020.

[16] I. Bakkouri and K. Afdel, "Mlca2f: Multi-level context attentional feature fusion for covid-19 lesion segmentation from ct scans," *Signal, Image and Video Processing*, vol. 17, no. 4, pp. 1181–1188, 2023.

[17] I. Bakkouri, K. Afdel, J. Benois-Pineau, and G. C. F. t. A. D. N. Initiative, "Bg-3dm2f: bidirectional gated 3d multi-scale feature fusion for alzheimer's disease diagnosis," *Multimedia Tools and Applications*, vol. 81, no. 8, pp. 10743–10776, 2022.

[18] I. Bakkouri and K. Afdel, "Computer-aided diagnosis (cad) system based on multi-layer feature fusion network for skin lesion recognition in dermoscopy images," *Multimedia Tools and Applications*, vol. 79, no. 29, pp. 20483–20518, 2020.

[19] I. Bakkouri and K. Afdel, "Multi-scale cnn based on region proposals for efficient breast abnormality recognition," *Multimedia Tools and Applications*, vol. 78, pp. 12939–12960, 2019.

[20] A. Saglietto, D. Baccega, R. Esposito, M. Anselmino, V. Dusi, A. Fiandrotti, and G. M. De Ferrari, "Convolutional neural network (cnn)-enabled electrocardiogram (ecg) analysis: a comparison between standard twelve-lead and single-lead setups," *Frontiers in Cardiovascular Medicine*, vol. 11, p. 1327179, 2024.

[21] U. R. Acharya, H. Fujita, O. S. Lih, M. Adam, J. H. Tan, and C. K. Chua, "Automated detection of coronary artery disease using different durations of ecg segments with convolutional neural network," *Knowledge-Based Systems*, vol. 132, pp. 62–71, 2017.

[22] J. Zhang, D. Liang, A. Liu, M. Gao, X. Chen, X. Zhang, and X. Chen, "Mlbf-net: A multi-lead-branch fusion network for multi-class arrhythmia classification using 12-lead ecg," *IEEE Journal of Translational Engineering in Health and Medicine*, vol. 9, pp. 1–11, 2021.

[23] B. Wang, G. Chen, L. Rong, Y. Liu, A. Yu, X. He, T. Wen, Y. Zhang, and B. Hu, "Arrhythmia disease diagnosis based on ecg time–frequency domain fusion and convolutional neural network," *IEEE Journal of Translational Engineering in Health and Medicine*, vol. 11, pp. 116–125, 2023.

[24] A. Ullah, S. u. Rehman, S. Tu, R. M. Mehmood, Fawad, and M. Ehatisham-ul Haq, "A hybrid deep cnn model for abnormal arrhythmia detection based on cardiac ecg signal," *Sensors*, vol. 21, no. 3, p. 951, 2021.

[25] A. A. Ahmed, W. Ali, T. A. Abdullah, and S. J. Malebary, "Classifying cardiac arrhythmia from ecg signal using 1d cnn deep learning model," *Mathematics*, vol. 11, no. 3, p. 562, 2023.

[26] G. Petmezas, K. Haris, L. Stefanopoulos, V. Kilintzis, A. Tzavelis, J. A. Rogers, A. K. Katsaggelos, and N. Maglaveras, "Automated atrial fibrillation detection using a hybrid cnn-lstm network on imbalanced ecg datasets," *Biomedical Signal Processing and Control*, vol. 63, p. 102194, 2021.

[27] A. Phoemsuk and V. Abolghasemi, "Multi-disease cardiovascular detection from ecg signals using an attention-driven deep network," in *2025 47th Annual International Conference of the IEEE Engineering in Medicine and Biology Society (EMBC)*, IEEE, 2025.

[28] H. Li, X. Wang, C. Liu, Y. Wang, P. Li, H. Tang, L. Yao, and H. Zhang, "Dual-input neural network integrating feature extraction and deep learning for coronary artery disease detection using electrocardiogram and phonocardiogram," *IEEE Access*, vol. 7, pp. 146457–146469, 2019.

[29] U. R. Acharya, Y. Hagiwara, J. E. W. Koh, S. L. Oh, J. H. Tan, M. Adam, and R. San Tan, "Entropies for automated detection of coronary artery disease using ecg signals: A review," *Biocybernetics and Biomedical Engineering*, vol. 38, no. 2, pp. 373–384, 2018.

[30] B. Lal, D. R. Gopagoni, B. Barik, M. A. Khan, R. D. Kumar, and T. V. Lakshmi, "An efficient qrs detection and pre-processing by wavelet transform technique for classifying cardiac arrhythmia," *International Journal of Intelligent Systems and Applications in Engineering*, vol. 11, no. 8s, pp. 490–498, 2023.

[31] P. Tang, Q. Wang, H. Ouyang, S. Yang, and P. Hua, "The feasibility of early detecting coronary artery disease using deep learning-based algorithm based on electrocardiography," *Aging (Albany NY)*, vol. 15, no. 9, p. 3524, 2023.

[32] K. Karboub, M. Tabaa, F. Monteiro, S. Dellagi, F. Moutaouakkil, and A. Dandache, "Automated diagnosis system for outpatients and inpatients with cardiovascular diseases," *IEEE Sensors Journal*, vol. 21, no. 2, pp. 1935–1946, 2021.
[33] M. Dey, N. Omar, and M. A. Ullah, "Temporal feature-based classification into myocardial infarction and other cvds merging cnn and bi-lstm from ecg signal," *IEEE Sensors Journal*, vol. 21, no. 19, pp. 21688–21695, 2021.
[34] C.-J. Zhang, F.-Q. Tang, H.-P. Cai, and Y.-F. Qian, "Heart failure classification using deep learning to extract spatiotemporal features from ecg," *BMC Medical Informatics and Decision Making*, vol. 24, no. 1, p. 17, 2024.
[35] R. Veerarajanm and V. V., "Multimodal contrastive learning for optimized integration of ecg signals and clinical reports for arrhythmia classification bibtex," *Journal of Healthcare Engineering*, vol. 14, no. 453-463, p. 5802722, 2025.
[36] S. K. Bashar, M. B. Hossain, E. Ding, A. J. Walkey, D. D. McManus, and K. H. Chon, "Atrial fibrillation detection during sepsis: study on mimic iii icu data," *IEEE journal of biomedical and health informatics*, vol. 24, no. 11, pp. 3124–3135, 2020.
[37] A. Phoemsuk and V. Abolghasemi, "Coronary artery disease classification using one-dimensional convolutional neural network," in *2024 IEEE Conference on Artificial Intelligence (CAI)*, pp. 389–394, IEEE, 2024.
[38] S. Seoni, F. Molinari, U. R. Acharya, O. S. Lih, P. D. Barua, S. García, and M. Salvi, "Application of spatial uncertainty predictor in cnn-bilstm model using coronary artery disease ecg signals," *Information Sciences*, vol. 665, p. 120383, 2024.
[39] A. E. Johnson, T. J. Pollard, L. Shen, L.-w. H. Lehman, M. Feng, M. Ghassemi, B. Moody, P. Szolovits, L. Anthony Celi, and R. G. Mark, "Mimic-iii, a freely accessible critical care database," *Scientific data*, vol. 3, no. 1, pp. 1–9, 2016.
[40] N. Iyengar, C. Peng, R. Morin, A. L. Goldberger, and L. A. Lipsitz, "Age-related alterations in the fractal scaling of cardiac interbeat interval dynamics," *American Journal of Physiology-Regulatory, Integrative and Comparative Physiology*, vol. 271, no. 4, pp. R1078–R1084, 1996.
[41] M. Sharma and U. R. Acharya, "A new method to identify coronary artery disease with ecg signals and time-frequency concentrated antisymmetric biorthogonal wavelet filter bank," *Pattern Recognition Letters*, vol. 125, pp. 235–240, 2019.
[42] E. Butun, O. Yildirim, M. Talo, R.-S. Tan, and U. R. Acharya, "1d-cadcapsnet: One dimensional deep capsule networks for coronary artery disease detection using ecg signals," *Physica Medica*, vol. 70, pp. 39–48, 2020.
[43] R. Holgado-Cuadrado, C. Plaza-Seco, L. Lovisolo, and M. Blanco-Velasco, "Characterization of noise in long-term ecg monitoring with machine learning based on clinical criteria," *Medical & Biological Engineering & Computing*, pp. 1–14, 2023.
[44] H. Ghonchi, S. Ferdowsi, and V. Abolghasemi, "Common spatial pattern with deep learning for fetal heart rate monitoring," in *2022 IEEE Workshop on Signal Processing Systems (SiPS)*, pp. 1–6, 2022.
[45] R. Alcaraz, D. Abásolo, R. Hornero, and J. J. Rieta, "Optimal parameters study for sample entropy-based atrial fibrillation organization analysis," *Computer methods and programs in biomedicine*, vol. 99, no. 1, pp. 124–132, 2010.
[46] Y. Obeidat and A. M. Alqudah, "A hybrid lightweight 1d cnn-lstm architecture for automated ecg beat-wise classification.," *Traitement du Signal*, vol. 38, no. 5, 2021.
[47] Animikhaich, "Animikhaich/ecg-atrial-fibrillation-classification-using-cnn."

VAHID ABOLGHASEMI (Senior Member, IEEE) received the Ph.D. degree in signal processing from the University of Surrey, Guildford, U.K., in 2011. He is currently an Associate Professor with the School of Computer Science and Electronic Engineering, University of Essex, Colchester, U.K. His main research interests include signal and image processing, compressive sensing, and machine learning. His expertise extends to cutting-edge technologies, including smart and adaptive low-power sensing and communication, wireless image transmission, compressed and lightweight neural networks, and artificial intelligence.

ATITAYA PHOEMSUK (Student Member, IEEE) received an MSc degree in Artificial Intelligence from the University of Essex, Colchester, UK, in 2020. She is currently pursuing a Ph.D. at the School of Computer Science and Electronic Engineering, University of Essex, UK. Her research interests include signal processing, biomedical data analysis, and deep learning.